

3D Vascular Segmentation using MRA Statistics and Velocity Field Information in PC-MRA

Albert C. S. Chung¹, J. Alison Noble¹, Paul Summers² and Michael Brady¹

¹ Department of Engineering Science, Oxford University, Oxford, United Kingdom.
{albert,noble,jmb}@robots.ox.ac.uk

² Department of Clinical Neuroscience, King's College, London, United Kingdom.
p.summers@iop.kcl.ac.uk

Abstract. This paper presents a new and integrated approach to automatic 3D brain vessel segmentation using *physics-based statistical models* of background and vascular signals, and *velocity (flow) field information* in phase contrast magnetic resonance angiograms (PC-MRA). The proposed new approach makes use of realistic statistical models to detect vessels more accurately than conventional intensity gradient-based approaches. In this paper, rather than using MRA speed images alone, as in prior work [7, 8, 10], we define a 3D local phase coherence (LPC) measure to incorporate velocity field information. The proposed new approach is an extension of our previous work in 2D vascular segmentation [5, 6], and is formulated in a variational framework, which is implemented using the recently proposed modified level set method [1]. Experiments on flow phantoms, as well as on clinical data sets, show that our approach can segment normal vasculature as well as low flow (low SNR) or complex flow regions, especially in an aneurysm.

1 Introduction

Intracranial aneurysms are increasingly treated using an endovascular technique known as the Guglielmi detachable coil (GDC) method in which platinum coils are guided through the blood vessels for placement in an aneurysm to induce thrombosis. To increase the success rate and procedural safety of the treatment, radiologists need a comprehensive and patient-specific understanding of the 3D shape, size and position of each aneurysm as well as the vasculature in the vicinity of the aneurysm. This has created the need to develop 3D vascular reconstruction and analysis methods for Magnetic Resonance Angiograms (MRA).

Aneurysm segmentation is a more complicated problem than vascular segmentation. In particular, regions inside an aneurysm can exhibit complex flow pattern and low flow rate. These phenomena, which induce significant signal loss and heterogeneous signal level within the aneurysm, lower the visibility of the aneurysm and make segmentation difficult. Most prior vascular segmentation techniques [7, 8, 10], which use TOF-MRA or speed images from PC-MRA, are not sufficient to recover the complete shape of the aneurysm because the

aneurysm region does not always form a piecewise homogeneous intensity partition with sharp (intensity) boundaries. Equally, conventional edge-based methods often do not work well because the true vessel boundaries may not have a high signal-to-noise ratio (SNR) or intensity gradient. To overcome these problems, we propose an original approach to segmenting aneurysms, as well as normal vasculature, on the basis of original velocity field information (measured by *local phase coherence*, LPC) and a tailored statistical description of PC-MRA speed images. In this paper, we build on our previous work [5, 6] to pose 3D vascular segmentation as a variational problem. The implementation is realised using the modified level set method [1]. The new approach does not require intensity gradient information. Experiments on flow phantoms and on clinical data sets show that the new approach can achieve better quality segmentation in PC-MRA images than either the conventional intensity gradient-based approach, or an approach that uses PC-MRA speed images alone.

2 Segmentation using MRA statistics of the speed images

This section begins by discussing a potential problem of using intensity gradient-based techniques in MRA segmentation, and then goes on to present a new segmentation method using MRA statistics of speed images. Figure 1a shows a typical vessel cross-section and illustrates an example of segmentation using an intensity gradient-based approach in MRA speed images. Within a slice, the optimal contour is defined as $\min_C \int_C g \cdot ds$, [8, 9], where the intensity gradient function g is defined as $1/(1 + |\nabla G \otimes I|^2)$; the Gaussian variance was set to 0.5 in this implementation. The intensity gradient function tends towards zero in regions of high intensity gradient. It should be noted that the optimal contour lies inside the vessel rather than on the vessel boundary because the low SNR regions (near the boundary) cannot provide sufficiently high intensity gradient (Figure 1a).

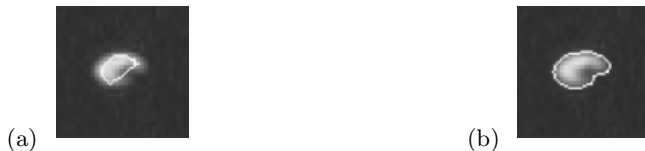


Fig. 1. Cross-sections of vessel and contours found by (a) intensity gradient-based approach and (b) a method using MRA statistics of the speed images

To counter this, we employ the statistical background and vascular signal models we developed in prior work [5, 6] for detecting vessel boundaries. Briefly, the models are based on the physics of MRA image formation and the assumption of laminar flow. We have shown that the background and vascular signal intensity values in speed images follow a Maxwell-Gaussian mixture distribution and uniform distribution respectively [6]. In this new method, S is defined

as a family of parametric surfaces. S is defined as $[0, 1] \times [0, 1] \times [0, \infty) \rightarrow \mathfrak{R}^3$ and $(\mathbf{q}, t) \rightarrow S(\mathbf{q}, t)$, where \mathbf{q} and t are the space and time parameters respectively. Suppose that P_v and P_b are the posterior probabilities of the vessel and background at each voxel respectively. A probabilistic energy functional is then defined as $E_s(t) = \int_{Inside\ S} -P_v \cdot dV + \int_{Outside\ S} -P_b \cdot dV$, where dV is a volume element. Minimising the probabilistic energy E_s amounts to finding an optimal surface in which the total posterior probability is maximum. Solving the Euler-Lagrange equation with the divergence theorem, the evolution equation of the surface S can be obtained. This is given by

$$\frac{\partial S}{\partial t} = (P_v - P_b) \cdot \hat{N}, \quad (1)$$

where \hat{N} is the unit outward normal of the surface S and $-1 \leq P_v - P_b \leq 1$. This equation governs the motion of geodesic flow towards the minimum and has been implemented using the modified level-set method [1]. Figure 1b illustrates the result obtained using the proposed new approach. It is a significant improvement compared with Figure 1a, as the detected boundaries are correctly placed on the true vessel boundaries.

3 LPC and integration with MRA statistics

PC-MRA generates a velocity field by measuring the three orthogonal phase shifts at each voxel. These are directly proportional to the corresponding speeds along the three directional components. By examining the velocity field, it has been observed experimentally that, within the vasculature, blood motion tends to be locally coherent [4]. In prior work we exploited this fact to propose a measure of 2D LPC as a constraint to improve the quality of vascular segmentation [6].



Fig. 2. (a) Speed and (b) LPC images

Specifically, 2D LPC is defined as follows: Given a 3x3 planar mask with a centre on voxel c and that each matrix element, except c , contains a normalised vector indicating the flow direction in 3D, eight pairs of adjacent 3D vectors are formed. The 2D LPC at c is the sum of the dot products of the eight adjacent vector pairs. 3D LPC is then defined as follows: Given three mutually orthogonal planes, three 3x3 planar masks are applied at c and three 2D LPC measures are obtained along each plane. The 3D LPC at c is the average of the three 2D LPC measures. Note that the higher the value, the more coherent the blood motion. Figure 2a shows a MRA speed image, in which the intensity values in the middle

of the vessel are low and some voxels have intensity values almost as low as the background. However, the 3D LPC image is more homogeneous, with the inside regions exhibiting high LPC values with small variance (Figure 2b).

We then combine the physics-based MRA statistics and velocity field information (measured by LPC) in PC-MRA data as follows. A LPC energy functional can be defined as $E_{lpc}(t) = \int_{Inside\ S} \frac{(P-\mu_i)^2}{N_i} \cdot dV + \int_{Outside\ S} \frac{(P-\mu_o)^2}{N_o} \cdot dV$, where P is the 3D LPC value, E_{lpc} is an energy term representing the total variance of LPC values, μ_i and μ_o are the means of LPC values, N_i and N_o are the number of voxels, subscripts i and o denote inside and outside the surface respectively.

To integrate MRA statistics and LPC, we define the total energy E_{total} as a weighted sum of the probabilistic energy E_S and LPC energy E_{lpc} , as given by $E_{total}(t) = W_s \cdot E_S(t) + W_{lpc} \cdot E_{lpc}(t)$, where W_s and W_{lpc} are weights attached to the energy terms. Using the Euler-Lagrange equation with the divergence theorem, we obtain the evolution equation of surface S , which is $\frac{\partial S}{\partial t} = (W_s \cdot F_S + W_{lpc} \cdot F_{lpc}) \cdot \hat{N}$, where $F_S \equiv P_v - P_b$ (*MRA Statistics Force*), $F_{lpc} \equiv \frac{(P-\mu_o)^2}{N_o} - \frac{(P-\mu_i)^2}{N_i}$ (*LPC Force*) and \hat{N} is the outward surface normal. To maintain similarity of forces and polarity of the LPC force, the LPC force is normalised so that it is dimensionless and its polarity is maintained. As such, the normalised LPC force is given by $F'_{lpc} = sign(F_{lpc}) \cdot \frac{|F_{lpc}|}{|F_{lpc}|_{max}}$. The equation of motion can then be re-expressed as:

$$\frac{\partial S}{\partial t} = (W_s \cdot F_S + W_{lpc} \cdot F'_{lpc}) \cdot \hat{N}, \quad (2)$$

where $-1 \leq F_S, F'_{lpc} \leq 1$. The weights need not sum to one and can be adjusted according to the application. Both were set to one in this implementation.

For this application, we used a sub-voxel level set method for accurate surface representation [1]. In addition, to avoid signed distance function re-initialisation, we maintained the signed distance function in every update of the surface by using the Fast Marching method to build the extension forces in all non-zero level sets. The level-set version of Eq. 2 is given by $\frac{\partial \phi}{\partial t} + (W_s \cdot F_S + W_{lpc} \cdot F'_{lpc}) \cdot |\nabla \phi| = 0$, where ϕ is the evolving level set function. We constructed the initial surface S_o near the optimal solution using global thresholding [5]. We have found that the convergence rate of the motion equation depends on the size of the aneurysm. The convergence of our implementation is usually reached within 30 iterations for a large aneurysm (12-25mm diameter) and more than 100 iterations for a giant aneurysm (> 25mm diameter).

4 Results

Phantom Study (I): The segmentation approach was validated using a geometrically accurate straight tube with an 8mm diameter (SST Phantom). The tube was scanned using a PC-MRA protocol on a 1.5T GE MR scanner. The data volume was 256x256x81 voxels with voxel dimensions of 0.625mm x 0.625mm x 1.3mm. The flow rate was constant (40cm/s). For ease of reference, we use

EDGE, STAT, STAT-LPC to refer to an intensity gradient-based approach, the approach using MRA statistics on speed images alone ($W_S = 1$ and $W_{lpc} = 0$ in Eq. 2), and the approach using MRA statistics and LPC respectively. All 3 approaches were implemented using the modified level set method and the same initial surface. The EDGE algorithm followed the method proposed by Lorigo et. al. [8]. As the tube diameter was known, detection accuracy could be quantified by an area measurement error, i.e. $[1 - (Area_{measured}/Area_{true})] \times 100\%$. The area measurement errors of EDGE, STAT and STAT-LPC are shown in Figure 3, in which smaller image slice numbers represent the inflow region of the tube. The SNR of the images decreases with increasing slice number due to progressive saturation of fluid. Also, it is known that imperfections in velocity encoding due to non-linearities in the gradient systems can cause a position dependent deviation in the velocity images [3]. These two factors may have influenced the behaviour of our segmentation method. Note that the area measurement error increases as the slice number increases, where the delineation of true boundary is adversely affected by the partial volume artifact and low SNR. Considering all slices of the tube, the average area measurement errors of EDGE, STAT and STAT-LPC were 34.77% , 16.11% and 12.81% respectively. This demonstrates that STAT-LPC gives more accurate vessel boundaries than EDGE or STAT.

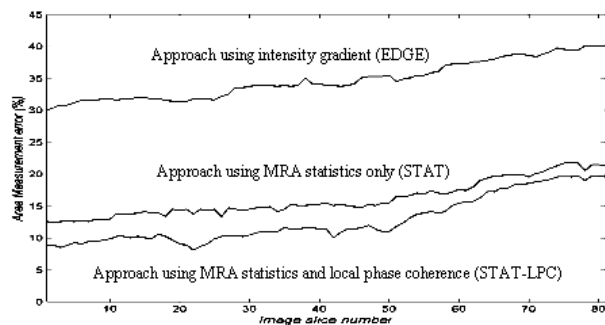


Fig. 3. The area measurement errors (see text for details)

Phantom Study (II): The approach was applied to an in-vitro silicon aneurysm model (Middle Cerebral Artery Bifurcation Aneurysm-MCA), as shown in Figure 4c. The model was scanned using the PC-MRA protocol as before. The data volume size 256x256x23 voxels with voxel dimensions of 0.8mm x 0.8mm x 1mm. Mean flow rate was set to 300 ml/min. Figures 4a and 5a show the 3D reconstruction and a cross-section of the MCA aneurysm respectively, in which the results of segmentation using MRA statistics on speed images alone are shown. Significant segmentation improvement is achieved using the segmentation method which utilises both MRA statistics and LPC, as shown in Figures 4b and 5b. The small circle in the middle of Figure 5b represents the singular point of the

velocity field, where the flow is almost zero. It does not affect the quality of visualisation in 3D because it lies inside the aneurysmal surface, and can easily be removed. Indeed, this is a useful feature to detect because it indicates to a radiologist the position of stagnant flow inside the aneurysm.



Fig. 4a. 3D reconstructed aneurysm model using MRA statistics alone



Fig. 4b. 3D reconstructed aneurysm model using MRA statistics & LPC

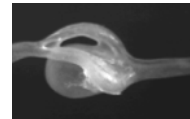


Fig. 4c. Digital camera view of the aneurysm model



Fig. 5a. Model

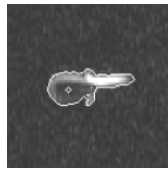


Fig. 5b. Model

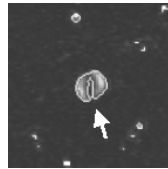


Fig. 6a. Patient 1

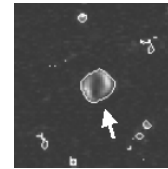


Fig. 6b. Patient 1

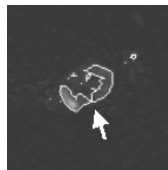


Fig. 7a. Patient 2

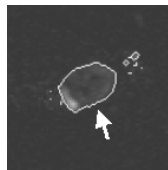


Fig. 7b. Patient 2

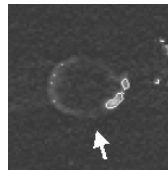


Fig. 8a. Patient 3

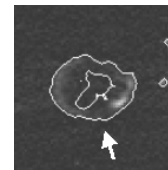


Fig. 8b. Patient 3

Case studies: Intracranial scans of 3 patients were acquired using the PC-MRA protocol as before. Each data set consists of 256x256x28 voxels of 0.8mm x 0.8mm x 1mm each. We compare segmentation using MRA statistics alone and using MRA statistics and LPC on the three volumes. As shown in Figures 6a, 7a and 8a, the segmentation with MRA statistics alone is good overall but fails in the middle of the aneurysms because of low blood flow, which cannot generate a sufficiently high intensity signal for vessel detection. Figures 6b, 7b and 8b show significant segmentation improvements using MRA statistics and LPC. As in the case of Figure 5b, the delineated contour in Figure 8b does not enclose the whole aneurysm. 2 major causes are likely. First, the flow rate inside the aneurysm was extremely low, which led to serious corruption of velocity field by noise. Secondly, a circular (or deformed circular) flow pattern was formed, which generated singularities in the aneurysm centre. These affect the LPC measure. However, Figure 8b represents a large improvement compared with Figure 8a, and the hole in the middle does not affect the quality of visualisation.

5 Conclusions

A new and integrated approach to automatic 3D brain vessel segmentation has been presented, which combines physics-based statistical models of background and vascular signals, and velocity (flow) field information in the PC-MRA data. In this paper, rather than using the MRA speed images alone, as in prior work [7, 8, 10], we have defined a local phase coherence measure to incorporate the velocity field information. The proposed approach has been formulated in a variational framework implemented using the modified level set method [1].

The proposed new approach was applied to two flow phantoms (a straight tube and an aneurysm model) and three clinical data sets. Using a geometrically accurate flow phantom, it has been shown that our approach can detect vessel boundaries more accurately than either the conventional intensity gradient-based approach, or an approach using MRA speed images alone. The results of experiments on an aneurysm model and clinical data sets show that our approach can segment normal vasculature as well as the low or complex flow regions, especially regions near vessel boundaries and regions inside aneurysms. Future studies will compare these segmentation methods on a larger number of clinical aneurysms.

Acknowledgements: AC is funded by a postgraduate scholarship from the Croucher Foundation, Hong Kong. JMB and JAN thank EPSRC for support. The authors would like to thank Prof. J. Byrne for clinical advice related to this work; Prof. D. Rufenacht and Dr. K. Tokunaga for making the aneurysm model; ISMRM Flow and Motion Study Group, Stanford CA for use of the SST phantom.

References

1. Adalsteinsson, D., Sethian, J.A.: The Fast Construction of Extension Velocities in Level Set Methods. *IJCP* **148** (1999) pp. 2-22
2. Andersen, A.H., Kirsch, J.E.: Analysis of noise in phase contrast MR imaging. *Med. Phys.* **23(6)** (June 1996) pp. 857-869
3. Bernstein, M.A., Zhou, X.J., et al.: Concomitant gradient terms in phase contrast MR: analysis and correction. *MRM* **39(2)** (Feb. 1998) pp. 300-308
4. Burleson, A.C., et al.: Computer Modeling of Intracranial Saccular and Lateral Aneurysms for the Study of Their Hemodynamics. *Neurosurgery* **37(4)** (95)774-84
5. Chung, A.C.S., Noble, J.A.: Statistical 3D vessel segmentation using a Rician distribution. *MICCAI'99* (1999) pp.82-89 and *MIUA'99* (1999) pp.77-80
6. Chung, A.C.S., Noble, J.A., et al.: Fusing Speed and Phase Information for Vascular Segmentation in Phase Contrast MR Angiograms. *MICCAI'00* (2000) pp.166-75
7. Krissian, K., Malandain, G., et al.: Model Based Detection of Tubular Structures in 3D Images. *INRIA-Technical Report* RR-3736 (1999)
8. Lorigo, L.M., Faugeras, O., et al.: Co-dimension 2 Geodesic Active Contours for MRA Segmentation. *IPMI'99* (1999) pp.126-139
9. Malladi, R., Sethian, J.A., et al.: Shape Modelling with Front Propagation: A Level Set Approach. *PAMI* **17(2)** (1995) pp.158-175
10. McNerney, T., Terzopoulos, D.: Medical Image Segmentation Using Topologically Adaptable Surface. *CVRMed'97* (1997) pp.23-32